Theoretical and Computational Analysis of Pulsed Plasma Thruster Plumes

Nikos A. Gatsonis* and Xuemin Yin†
Computational Gas & Plasma Dynamics Laboratory
Mechanical Engineering Department
Worcester Polytechnic Institute
Worcester, MA 01609

Abstract

Pulsed Plasma Thruster (PPT) plume characteristics and modeling issues are discussed. A hybrid plume model is derived based on a particle description of neutrals and ions and a fluid description of electrons. Electric fields are obtained from a charge conservation equation under the assumption of quasineutrality. An axisymmetric, hybrid numerical code is developed based on a combination of DSMC, PIC and fluid computational techniques. The code incorporates a dual-grid structure, sub-cycling for the time integration, and time-varying particle injection. The No-Time-Counter methodology is used for neutral-neutral, elastic ion-neutral, and charge exchange collisions. Ion-electron collisions are modeled with the use of a collision force field. A typical simulation of a PPT plume is presented. The results demonstrate the expansion of the neutral and ion components of the plume and the generation of a low energy ion population due to charge exchange reactions.

Introduction

Pulsed plasma thruster (PPT) is an electromagnetic thruster that uses solid Teflon for propellant. PPTs can deliver high specific impulses of up to 1000 s, have low electric power requirements (<150 W), small size and weight, and a very simple propellant system. These characteristics make them an attractive and reliable on-board propulsion alternative. Potential applications include orbit maintenance, attitude control, orbit insertion and de-orbiting for both large and small satellite missions. As with any propulsion technology, successful integration and operation of PPTs on spacecraft require the complete assessment of the environment induced by PPT plumes, as well as the potential for spacecraft interactions. The characteristics of PPT plumes are quite distinct when compared to other electric or chemical thrusters. PPTs produce thrust by the acceleration of ablated Teflon during a pulsed discharge of an energy storage capacitor. The arc discharge lasts several microseconds and ablates several micrograms of the Teflon propellant. The force resulting from the interaction between the current and the induced magnetic field accelerates the generated plasma outside the thruster. Only a portion of the ablated mass becomes ionized. Therefore, PPT plumes are composed of various ion and neutral species due to propellant decomposition. In addition, they contain non-propellant efflux due to thruster materials, electromagnetic efflux and optical emissions. PPT plumes are inherently unsteady created by the interaction of individual plasmoids during the pulsed operation of the thruster. Physical modeling of PPT plumes is very limited and simulation of such a partially ionized, collissional, and high-density plasma is very challenging. Because of the projected use of PPTs it is important to further investigate their plumes and develop a predictive ability that will determine the potential for spacecraft interactions. The motivation of our study is to develop a physical and computational model capable of addressing the PPT effluent environment where both the neutral and plasma dynamics and transport are important. The modeling effort is in close interaction with the plume characterization efforts at LeRC and will provide the much-needed predictive capability.

In this paper we review first the background on PPT effluents and the computational issues involved in PPT plume modeling. We then present the physical model, which is based on a hybrid description of the plasma. We summarize the hybrid computational methodology that combines concepts from the Direct Simulation Monte Carlo (DSMC), the Particle-in-Cell (PIC) and fluid techniques. We finally present a sample result while in a companion paper (*Yin* and *Gatsonis*, 1997) we present details from PPT plume simulations.

PPT Plume Effluents

A review of the PPT literature reveals an early awareness for the assessment of plume contamination. PPT plume characterization has been challenging since it requires development of special diagnostic techniques to cope with the intricacies of the plume. The majority of the available ground-based investigations was conducted in the early 1970's using the LES-6 thruster

* Assistant Professor, CGPL, Mechanical Engineering Department, WPI, 100 Institute Rd., Worcester, MA, 01609.

† Graduate Research Assistant, CGPL, Mechanical Engineering Department, WPI, 100 Institute Rd., Worcester, MA, 01609.

[*Vondra et al.*, 1970; *Vondra et al.*, 1971; *Thomassen* and *Vondra*, 1972; *Thomassen* and *Tong*, 1973] or specifically designed PPTs [*Guman* and *Begun*, 1977; *Rudolph et al*, 1979]. Few studies appeared in the 1980's [*Drawbarn et al.*, 1982; *Hirata* and *Murakami*, 1984]. The renewed interest in PPTs prompted new plume investigations using a derivative of the flight-qualified LES-8/9 [*Myers* et al, 1996; *Eckman* et al., 1997]. As a result of these experimental investigations various aspects of PPT plumes and contamination issues have been addressed.

PPT plumes consist of single- and multiple-ionized species, as well as neutrals, resulting from the partial decomposition of Teflon. In addition, particles from eroded thruster materials have been identified in the plume. Species production in the PPT channel is time dependent and species populations have different characteristics (mean velocity and temperature). Despite the numerous ground-based investigations the characterization of the plume species is far from being complete. Fast moving ions appear to explain the thrust derived by PPTs but there is little information on the relevant contribution of the multiple-ionized components of the charged efflux. It has been established that neutral particles continue to leave the thruster well after the passage of ions, but there is a fast moving neutral component as well. Analysis indicates that a significant fraction of the plume mass is relatively slow moving and at low temperature. Therefore, gasdynamic effects related to the low energy portion of the plume can be important on the backflow of material. The exact composition of the neutral efflux or their contribution to the thrust is still unanswered questions. Overall, the composition of the plume depends strongly on thruster operating conditions. Possible chemical interactions in the plume have not been investigated so far. The plume potential for spacecraft interactions depends on the characteristics of each particle population: the high-energy particles, for example, can not contribute to spacecraft interactions unless they are impinging spacecraft surfaces directly. However, secondary interactions that lead to the generation of low energy species need to be investigated. Such interactions include charge-exchange reactions, which have been thoroughly studied in ion thrusters but not for PPTs. It should be pointed out that the extensive flight heritage of PPTs showed no adverse effects on spacecraft operation. The NOVA PPTs (peak power level of 30 W, I_{sp} of 543 s and I_{bit} of 400 μN-s) with a combined operation of over 20 years showed no observed impact on solar arrays or other spacecraft operations [*Ebert* et al., 1989]. The Lincoln Experimental Satellite (LES) launched in 1968 used flawlessly four experimental PPTs for station keeping for almost 9000 hours [*Guman* and *Nathanson*, 1970]. However, ground-based and flight results cannot be scaled easily to new designs or more powerful PPTs planned for future missions. It is also important to note that current spacecraft designs, sensors and operations may be fundamentally different from those in the early demonstration flights.

Modeling Issues and Methodology

Based on our current understanding it can be argued that plumes from PPTs are more complex than other electric or chemical thrusters due to the presence of a neutral and an ionized component as well as their unsteady character. The physical modeling of PPT plumes is also very limited and so far has been the indirect result of the experimental characterization efforts or internal PPT models. The partially ionized and unsteady nature of PPT plumes makes their simulation very challenging. PPT plumes fall in the category of high-density, collisional, partially ionized plasmas. Computational methodologies that treat the neutral and ionized components and their interactions are still under development. Currently, no comprehensive modeling capability exists that could be applied directly to PPT plumes.

Simulation of neutral plumes is a very mature field with Navier-Stokes solvers covering the continuum regime, and Direct Simulation Monte Carlo (DSMC) solvers covering the transitional to rarefied regimes. The DSMC method developed by *Bird* (1994) treats non-equilibrium effects, backflow, chemical reactions, and surface interactions very effectively (*Elgin et al.*, 1990; *Boyd et al.*, 1991; *Chung et al.*, 1993; *Woronowicz* and *Rault*, 1994; *Gatsonis et al.* 1996). Computational studies of fully ionized collisionless plasma plumes have used primarily the Particle-in-Cell method [*Birdsall* and *Langdon*, 1985; *Hockney* and *Eastwood*, 1988). To alleviate difficulties associated with electron time-steps, various formulations of PIC/Fluid (hybrid) methodologies have been developed and used in a variety of problems. Recently, such hybrid methodologies have been used successfully in the simulation of ion thruster plumes (*Samanta Roy, et al.*; 1996 a,b). A simulation methodology applicable to partially ionized plasmas is the PIC-Monte Carlo (PIC-MCC) [*Birdsall*, 1991]. The method is strictly applicable to low plasma densities due to Debye length limitations and to problems where neutral densities dominate the flow. In addition, the method is limited due to the lack of a kinetic description of the neutrals. The DSMC method has also been used to model flows with ionization (*Carlson* and *Hassan*, 1992; *Bartel* and *Justiz*, 1993; *Taylor et al.*, 1994). In most of these cases simple models for the plasma flow have been used. Problems with the DSMC relate to the treatment of electrons, as well as the modeling of charged particle collisions. In addition to the Monte Carlo extensions to PIC, many variations of hybrid (particle/fluid) approaches have been proposed for the intermediate regime between the collisionless and Coulomb dominated plasmas [*Jones et al.*, 1996]. Finally, purely fluid approaches have been used to address large-scale plasma jets [*Gatsonis* and *Hastings*, 1991; 1992]. Of course, as with any fluid description, the major shortcoming comes from the loss of the kinetic description of the flow.

In this study we present the first comprehensive physical and computational model of a PPT plume. The physical model is based on the understanding gained from the experimental investigations. The unsteady character of the plume is considered as a series of plasmoids ejected from the exit of the thruster channel during the thruster firing. The plume model includes neutrals (C, F, C_xF_y), ions ($C^+, F^+, C_x^+F_y^+$) from the Teflon decomposition and trace species from surface materials. A hybrid representation is chosen to model the physical characteristics of the PPT effluents. Neutrals and ions are treated as particles in order to obtain fluxal properties needed for contamination characterization. Electrons are treated as fluid. Charge exchange interactions are included in order to assess the potential for generation of a low-energy charge exchange plasma.

Our numerical model is also based on a hybrid approach that results in a novel combination of DSMC, PIC and fluid computational techniques. The code incorporates a dual-grid structure and sub-cycling for the time-integration. The inclusion of unsteady particle injection schemes allows for input from internal PPT models, experimental data and analytical models. Collisional interactions between charged and neutral species and chemical interactions are included using DSMC and hybrid collisional methodologies. For the model to be applicable to plasma flows where the magnitudes of Debye lengths restrict practical computations a quasineutral approach is adopted. Preliminary numerical simulations revealed basic features observed in PPT plumes.

Physical Model

The development of a theoretical model is based on the understanding of the effluxes present in PPT plumes. The simulation domain is an axisymmetric region shown in Figure 1. The downstream (axial direction) is designated by z and the radial direction by r. The bottom boundary is the centerline of the plume and is the axis of symmetry. The downstream, top, and upstream boundaries are placed at distances far enough to include the plume and to account for the investigation of backflow. The left (upstream) and top boundaries represent the far-field background plasma. At the thruster exit particles enter the domain with prescribed density, velocity or flux distributions. These profiles can be specified from either experimental observations or internal flow models. Species in the model include: (1) neutrals; (2) ions (3) charge-exchange ions; (4) electrons; (5) trace species. The charging of the top channel surface is not accounted for in this model.

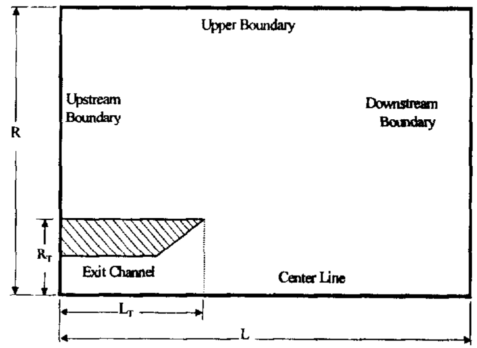

Figure 1. Physical Domain

In the hybrid formulation ions and neutrals are considered as particles and electrons as a massless fluid. The distribution function of a plume species s (i,n) with mass m_s is given by a local Maxwellian

$$f_s(\mathbf{r},\mathbf{v},t) = n_s(\mathbf{r},t)\left(\frac{m_s}{2\pi kT_s}\right)^{3/2} \exp\left[-\frac{m_s(\mathbf{v}_s-\mathbf{u}_s)^2}{2kT_s}\right] \quad (1)$$

where, $n_s(\mathbf{r},t)$ is the number density, $\mathbf{u}_s(\mathbf{r},t) = \langle \mathbf{v}_s \rangle \equiv (U_s, V_s, W_s)$ is the average (or drift) species velocity (brackets indicate average over the species distribution function) and T_s is the temperature. The typical range of parameters is shown in Table 1.

Table 1. Range of plume parameters

	Neutrals	Ions
T(eV)	≤ 6	≤ 6
n (m^{-3})	$\leq 10^{22}$	$\leq 10^{21}$
U(km/s)	0-5	10-60

Ions

For an ion particle with mass m_i charge q_i, particle velocity $\mathbf{v}_i$ and position $\mathbf{x}_i$ the equations of motion can be written as

$$m_i \frac{d\mathbf{v}_i}{dt} = q_i\mathbf{E} + \mathbf{F}_{ie} \qquad \frac{d\mathbf{x}_i}{dt} = \mathbf{v}_i \quad (2)$$

where $\mathbf{E}$ is the electric field and $\mathbf{F}_{ie}$ is the collision force given by *Jones et al.* [1996] as

$$\mathbf{F}_{it}(\mathbf{r},t) = \nu_{it} m_{it} (\langle \mathbf{v}_i \rangle - \langle \mathbf{v}_t \rangle) + \nu_{it}^E \frac{(T_i - T_t)}{\langle \mathbf{v}_i^2 \rangle - \langle \mathbf{v}_i \rangle^2} - \nu_{it} \frac{m_{it}^2 (\langle \mathbf{v}_i \rangle - \langle \mathbf{v}_t \rangle)^2}{\langle \mathbf{v}_i^2 \rangle - \langle \mathbf{v}_i \rangle^2} (\langle \mathbf{v}_i \rangle - \langle \mathbf{v}_t \rangle) \quad (3)$$

Ions in the model include the primary beam and charge-exchange (CEX) created by the following resonant charge-exchange reactions between slow neutrals and fast ions:

$$X^n_{slow} + X^+_{fast} \longrightarrow X^n_{fast} + X^+_{slow} \quad (4)$$

These relatively low-speed CEX ions can be strongly affected by the self-induced electric fields in the plume. As a result they can accelerate outside the plume in the radial and the backflow directions [*Samantha Roy et al.*, 1996 a,b]

Neutrals

Neutral species in the plume are modeled as particles following the DSMC methodology [*Bird*, 1994].

Fluid Electron Model

The steady electron momentum equation in the absence of magnetic field is

$$\mathbf{u}_e = -\frac{e\mathbf{E}}{m_e \nu_e} - \frac{1}{n_e m_e \nu_e} \nabla p_e + \frac{\sum_i \nu_{ei} \mathbf{u}_i}{\nu_e} + \frac{\sum_n \nu_{en} \mathbf{u}_n}{\nu_e} \quad (5)$$

The electron pressure is given by the ideal law, $p_e = n_e k T_e$, where k is the Boltzmann constant. The electron collision frequencies ν_{ei}, ν_{en} are given by *Burgers* [1967] and the total collision frequency is defined as

$$\nu_e = \sum_i \nu_{ei} + \sum_n \nu_{en} \quad (6)$$

Neglecting viscous terms ($\overline{\overline{\tau}}_e = 0$) and heat conduction ($\overline{\overline{q}}_e = 0$), the energy equation is

$$\frac{\partial}{\partial t}\left(\frac{3}{2} p_e\right) + \mathbf{u}_e \cdot \nabla \left(\frac{3}{2} p_e\right) + \frac{5}{2} p_e \nabla \cdot \mathbf{u}_e = \sum_t n_s \frac{m_s}{m_s + m_t} \nu_{st} \left[3k(T_t - T_s)\right] \Psi_{st} + m_t (\mathbf{u}_s - \mathbf{u}_t)^2 \Phi_{st} \quad (7)$$

The correction terms Φ_{st}, Ψ_{st} account for relative drifts between the species [*Burgers*, 1967; *Schunk*, 1977].

Current Conservation

The total current density is given by

$$\mathbf{J} = \sum_s n_s q_s \mathbf{u}_s = \sum_i n_i q_i \mathbf{u}_i - e n_e \mathbf{u}_e \quad (8)$$

One of the most important simplifications in the model comes from the assumption of quasi-neutrality, i.e., $\rho_c \approx 0$, where $\rho_c = \sum_s q_s n_s$ is the charge density. This approximation is valid for length scales that are much larger than the Debye length, λ_D. For plasma densities $n_e \approx 10^{16} - 10^{21}\,\mathrm{m^{-3}}$ and $T_e \approx 5\,\mathrm{eV}$, $\lambda_D \approx 10^{-4} - 10^{-7}\,\mathrm{m}$. This assumption is valid for the dense portions of the plume but it is certainly violated near solid walls or the edges of the plume. The electron density in the quasineutral approximation is simply given by

$$n_e \cong \sum_i n_i \quad (9)$$

The charge conservation equation under quasineutrality can be written as

$$\nabla \cdot \mathbf{J} = 0 \quad (10)$$

or using Eq. (5) and Eq. (8)

$$\nabla \cdot \left(\frac{e^2 n_e}{m_e \nu_e} \mathbf{E}\right) = -\nabla \cdot \mathbf{J}^I - \nabla \cdot \mathbf{J}^P - \nabla \cdot \mathbf{J}^{IC} - \nabla \cdot \mathbf{J}^{NC} \quad (11)$$

where

$$\mathbf{J}^I = \sum_i n_i q_i \mathbf{u}_i \quad (12)$$

$$\mathbf{J}^E = \frac{e^2 n_e}{m_e \nu_e} \mathbf{E} \qquad \mathbf{J}^P = \frac{e}{m_e \nu_e} \nabla p_e \quad (13)$$

$$\mathbf{J}^{IC} = -e n_e \frac{\sum_i \nu_{ei} \mathbf{u}_i}{\nu_e} \qquad \mathbf{J}^{NC} = -e n_e \frac{\sum_n \nu_{en} \mathbf{u}_n}{\nu_e} \quad (14)$$

We also neglect displacement currents in the plasma and induced magnetic fields. Therefore, electric fields are electrostatic given by a potential ϕ as

$$\mathbf{E} = -\nabla \phi \quad (15)$$

The boundary condition at the thruster exit can be derived from the exit flow conditions. For example, for zero total current density the electric field can be derived analytically using equations (12-14). Zero axial field is imposed along the downstream boundary and zero radial field along the axis centerline. In the backflow region the potential is set to zero. Along the top surface either a constant potential or zero field is imposed. Future extensions of the model will include a simple charging model for this surface.

Transport Properties

(1) Neutral-neutral collisions

The Variable Hard Sphere (VHS) model is used to model neutral-neutral collisions. The total cross section is

$$\sigma_T = \pi d_{ref}^2 \left(\frac{g_{ref}}{g}\right)^{2\omega - 1} \quad (16)$$

where d_{ref} is the reference diameter and ω the viscosity coefficient [*Bird*, 1994]. The mean collision frequency is given by

$$\nu_{nn} = n \sigma_{T,ref} g_{ref}^{2\omega-1} \frac{2}{\sqrt{\pi}} \Gamma(5/2 - \omega) \left(\frac{2kT_n}{m_r}\right) \quad (17)$$

(2) Ion-neutral collisions

The dominant collision processes in a weakly ionized plasma are two types of collisions between ion and neutral particles: the first is the non-resonant elastic collision for temperatures bellow 500°K; the second is the resonant collision with charge exchange. For non-resonant ion-neutral collisions, the momentum transfer cross section can be expressed as (*Banks,* 1966; *Dalgarno et al.*, 1959)

$$\sigma_M(g) = 2.21\pi\sqrt{\frac{\alpha\ e^2}{\mu_{in} g^2}} \quad (18)$$

in cm^2, where α is the polarizability of the neutral atom (in cm^3) and μ_{in} is the reduced mass. The average momentum transfer collision frequency can be simplified to

$$\nu_{in} = 2.586\times 10^{-16} n_n \sqrt{\frac{\alpha_0}{\mu_A}} \quad (19)$$

where, n_n is the neutral number density (in m^{-3}) , μ_A is the reduced mass (in atomic mass units), and α_0 = $\alpha\times 10^{24}$ (cm^3).

The charge exchange reaction is expressed in Eq. (4) and *Dalgarno et al.* (1966) suggested a momentum transfer cross section in the form of

$$\sigma_M = 2(A - B\lg\varepsilon)^2 \quad (20)$$

where ε is the relative energy and A and B are constants determined by experimental data. The corresponding average cross section is:

$$\overline{\sigma}_{M,in} = 2\times 10^{-6}\left[(A + 3.96B) - B\log(T_i + T_n)\right]^2 \quad (21)$$

and the average collision frequency is

$$\nu_{in} = \frac{4}{3}\overline{\sigma}_{M,in} n_n \sqrt{\frac{8k}{\pi m}(T_i + T_n)} \quad (22)$$

(3) Charged particle collisions

The collision frequencies between particles s and t with drifting Maxwellian distributions needed in the evaluation of the force in Eq. (3) are derived by several authors [*Burgers*, 1969; *Schunk*, 1975]. For example, the average momentum transfer collision frequency is

$$\nu_{st} = \frac{16\sqrt{\pi}}{3} n_t \frac{m_t}{m_s + m_t}\left(\frac{\mu_{st}}{2kT_{st}}\right)^{\frac{3}{2}}\left(\frac{q_s q_t}{\mu_{st}}\right)^2 \ln\Lambda \quad (23)$$

where Λ is the Coulomb logarithm. Similar expressions can be found for the energy transfer collision frequency.

PPT Injection

Particle injection at the PPT exit requires the complete knowledge of the species distribution functions. Ideally this should be given from PPT thruster exit data or internal modeling. The total neutral and ion mass through the exit during a pulse is

$$M_{N(I)} = \sum_{n(i)} M_{n(i)} \quad (24)$$

and the total mass

$$M = M_I + M_N \quad (25)$$

Assuming that the total number density $n_{N(I)}$ is uniformly distributed along the thruster exit the species number density can be expressed using the species number fraction X_s as

$$n_{n(i)}(\mathbf{r}_e, t) = X_{n(i)} n_{N(I)}(t) \quad (26)$$

Assuming that for a species s the distribution at the exit is described by a drifting Maxwellian then the total neutral (or ion) mass injected is given as

$$M_{N(I)} = \frac{A}{4}\left[\sum_{n(i)} X_{n(i)} m_{n(i)} \bar{c}_{n(i)} F(s_{n(i)})\right]\int_{t_1}^{t_2} n_{N(I)}(t)\,\mathrm{d}t \quad (27)$$

where the average thermal speed is $\bar{c}_s = \sqrt{8kT_s/\pi m_s}$, $s_s = u_i/\sqrt{2kT_s/m_s}$,and

$$F(s_s) = \exp(-s_s^2) + \sqrt{\pi}s_s[1 + \mathrm{erf}(s_s)]$$

Assuming that some of the parameters $\mathbf{u}_i$, T_i, M, M_I (or Q) are given from measurements or simple thrust-balance models, then manipulation of Eqs. (24-27) can provide the number densities. The species distribution functions at the exit are then completely defined and all fluxal quantities can be evaluated.

Numerical Implementation

The numerical implementation of the previously described physical model is based on a hybrid approach and is summarized bellow.

Grid Structure

A structured rectangular grid is used in the code based on the estimate of the smallest mean-free path, λ_{st}. The vertices of each cell are the nodes where the charge and average (fluid) quantities are evaluated. A dual-grid structure may be used alternatively.

Particle Injection and Loading

The number of particles to be injected in a computational cell can be obtained once the distribution functions at the exit are determined. This computation is performed at each time step to reproduce the unsteady injection process. The same procedure is used to establish the ambient injection at the boundaries of the domain. The loading of the follows standard procedures as described by *Bird* (1994) or *Birdsall* and *Langdom* (1992). Particles reaching the far-field boundaries from inside the domain are removed from the simulation. The top surface of the channel is set to an "absorption" condition where the particles are assumed to be deposited onto the surface.

Collision Methodology

(1) Neutral-Neutral Collisions

The modeling of neutral particle motion and collisions is accomplished by the non-time-counter (NTC) method described by *Bird* (1994). A set of representative collision pairs between species p and q for each time step is chosen in each cell based on

$$N_C = 1/2 N_p \overline{N}_q W_N \left[(\sigma_T g)_{\max}\right]_{pq} \Delta t / V_C \quad (28)$$

For each selected pair, a collision is established based on the acceptance-rejection of the probability ratio defined as

$$\frac{\sigma_T g}{\left[(\sigma_T g)_{\max}\right]_{pq}} \quad (29)$$

The maximum value in the above expression is updated during the simulation. These steps are repeated until all collisions have been performed. Linear momentum and energy conservation equations are used in the evaluation of the post-collision velocities of the particles and the deflection angle is sampled from a uniform distribution. When multi-atomic molecules are included in the plume, the internal energy of the collision partners is re-distributed following the Larsen-Borgnakke model (*Bird*, 1994).

(2) Ion-Neutral Elastic Collisions

These collisions are treated as the *n-n* ones using the NTC model. The cross section used in the determination of the collision probability is given in Eq. (16). The occurrence is based on the available relative energy, which has to be below a specified threshold E_{cx}.

(3) Ion-Neutral Charge-Exchange Collisions

Normally, close to the exit the relative energy level of the plume ions is high enough for the occurrence of resonant charge-exchange collisions. The NTC model is used to determine the number of possible CEX partners in each cell with the cross section given in Eq. (20). Due to the nature of the charge-exchange collision, the post collision velocities of the reacting particles are simply exchanged.

(4) Ion-electron Collisions

These collisions are modeled by the collision force field discussed earlier.

Particle Mover

After the collision process has been completed in all cells, the particles are moved according to their post-collision velocities. The integration of the equation of motion of a neutral or an ion particle in axisymmetric coordinates must take into account the azimuthal component of the velocity following a procedure similar to the one described by *Birdsall and Langdom*, (1992) or *Bird* (1994).

The electric field is obtained from finite-differencing of Eq. (11). The charge n_i on the nodes is obtained through weighting of the charge of the particles found in the cells surrounding the node. In order to conserve charge in axisymmetric coordinates the weighting scheme of *Ruyten* [1993] is used. For ions, the electric field **E** and collisional force $\mathbf{F}_{ie}$ is interpolated at the particle position $\mathbf{x}_s$ using the same axisymmetric weighting scheme. Stability considerations for the integration of particle equations of motion are discussed in *Birdsall and Langdom*, (1992).

Results and Discussion

Results from a typical simulation are given in Figures 2-5. A simpler version of the model equations is used in the simulation based on the assumption of ambipolar diffusion (details can be found in our companion paper, *Yin and Gatsonis*; 1997). The data correspond to the LES-8/9 PPT: M=30 µg, M_I=7.5 µg, U_I=40 km/s, T_I=5 eV, T_N=5 eV, and period P=12 µs. Species fractions are $X_{C^+} = X_{F^+} = 0.5$ and $X_C = X_F = 0.5$.

Figure 2 shows that at t=12 µs the ion cloud has passed the downstream boundary. A component of backflow appears, as well as significant expansion in the radial direction. Figure 3 shows that at t=12 µs the neutral cloud has expanded and developed a cloud structure with radial and backflow components. Clearly this expansion implies that axial mean velocities are larger than the values found at the exit plane. Figures 4 and 5 display the phase plots ($v_{iz} - v_{ir}$) of the ion and neutral distribution functions. At t=12 µs the appearance of a second ion population is depicted in Fig. 4. This population is centered at about $U_i \approx 10\,\text{km/s}$ and has a significant spread. This population is a result of the charge exchange reactions between C-C^+ and F-F^+. As a result of the radial electric fields, the ionic population with large radial velocities increases. In addition, there appears to be ions with negative axial velocities. These backstreaming ions belong to the low energy population exclusively, as Fig. 4 shows. Figures 5 shows a similar phase plot for the neutrals. The neutrals injected with zero drift develop a population of high axial velocities (~40 km/s) due to charge exchange. In addition, neutrals expand in the radial direction as Fig. 5 depicts. As with the ions, at t=12 µs neutral backflow is predicted due to the population with negative axial velocities. An expanded set and details of plume simulations are presented in *Yin and Gatsonis* (1997).

Summary

In this study the first comprehensive physical and computational model for PPT plumes was presented. The hybrid theoretical model includes: ion and neutral particles; fluid electrons; a charge conservation equation; neutral-neutral, neutral-ion, charge exchange, and charged particle collisions. The hybrid computational methodology for the partially ionized PPT plume is based on a combination of the DSMC, PIC and fluid approaches. A sample calculation revealed important characteristics of the expanding neutral and ion components of the PPT plume.

Acknowledgments

This work was performed under grant NAG3-1873 sponsored by NASA Lewis.

References

1) Banks, P., *Collision frequencies and energy transfer: electrons*, Planet.Space Sci., 14:1085, 1968.
2) Banks, P., *Collision frequencies and energy transfer: ions*, Planet.Space Sci., 14:1104, 1968.
3) Bartel, T.J., Justiz, C.R., *DSMC simulation of ionized rarefied flows*, AIAA Paper 93-3095, 1993.
4) Bird, G.A., *Thermal and pressure diffusion effects in high altitude flows*, AIAA Paper 88-2732, June, 1988
5) Bird, G.A., *Molecular gas dynamics and the direct simulation of gas flows*, Clarendon Press, Oxford, 1994
6) Birdsall, C.K., *Particle-in-cell charged-particle simulations plus Monte Carlo collisions neutral atoms*, PIC-MCC, IEEE Transactions on Plasma Sci., Vol.19, No.2, April, 1991
7) Birdsall, C.K., Langdon, A.B., *Plasma physics via computer simulation*, McGraw-Hill, New York, 1992
8) Boyd, I.D., Penko. P.F., Meissner, D.L., *Numerical and experimental investigations of rarefied nozzle and plume flows of Nitrogen*, AIAA Paper 91-1363, June, 1991.
9) Burgers, J.M., *Flow Equations for Composite Gases*, Academic Press, 1969.
10) Carlson, A.B., Hassan, H.A., *Direct simulation of re-entry flows with ionization*, J. of Thermophysics and Heat Transfer, Vol.6, No.3, July-Sept., 1992, pp400-405
11) Chung, C.H., Kim, S.C., Stubbs, R.M., De Witt, K.J., *Analysis of plume backflow around a nozzle lip in a nuclear rocket*, AIAA Paper 93-2497, 1993
12) Dalgarno, A., McDowell, M.R., Williams, A., *The mobilities of ions in unlike gases*, Proc. R. Soc., A250:411, 1958
13) Dawbarn, R., McGuire, R.L., Steely, S.L., Pipes, J.G.,
14) *Operating characteristics of an ablative pulsed plasma engine*, AEDC TR-82-9.
15) Ebert, W.L., Kowal, S.J., Soan, R.F., *Operational Nova Spacecratf Teflon PPT System*, AIAA-89-2497,1989.
16) Eckman, R., Gatsonis, N., Myers, R., Pencil, E., *Experimental Investigation of the LES 8/9 Pulsed Plasma Thruster Plume*, IEPC-97-146.
17) Elgin, J.B., Cooke, D.C., Tautz, M.F., Murad, E., *Modeling of atmospherically induced gas phase optical contamination for orbiting spacecraft*, J. Geophys. Res., Vol.95, No.A8, Aug., 1990, pp12197-12208
18) Gatsonis, N.A., Hastings, D.E., *Evolution of the plasma environment induced around spacecraft by gas releases: three-dimensional modeling*, J. Geophys. Res., Vol.97, No.A10, Oct., 1992, pp14989-15005
19) Gatsonis, N.A., Buzby, J., Yin, X., Mauk, B.H., *Modeling nuclear thermal rocket plume effluents*, AIAA Paper 96-1850, 1996
20) Guman, W.J., Begun, M., *Pulsed plasma plume studies*, Air Force Rocket Propulsion Laboratory, TR-77-2, 1977
21) Guman, W.J., and Nathanson, D.M., *Pulsed Plasma Microthruster Propulsion System for Synchronous Orbit Satellite*, J. Spacecraft, V. 7, No. 4, 1970.
22) Hirata, M., Murakami, H., *Exhaust gas analysis of a pulsed plasma engine*, IEPC - 84-52, 1984.
23) Hockney, R.W., Eastwood, J.W., *Computer simulation using particles*, Adam Hilger, New York, 1988.
24) Jones, M.E., Lemons, D.S., Mason, R.J., Thomas, V.A., Winske, D., *A grid-based Coulomb method for PIC codes*, J. of Comp. Phys., Vol.123, 1996, pp169-181.
25) Mitchner, M., Kruger, C.H., Jr., *Partially ionized gases*, John Wiley & Sons, 1992.
26) Myers, R.M., Arrington, L.A., Pencil, E.J., Carter, J., Heminger, J., Gatsonis, N.A., *Pulsed plasma thruster contamination*, AIAA-96-2729, 1996.
27) Rudolph, L.K., Harstad, K.G., Pless, L.C., Jones, R.M., *Plume characterization of a one-millipound solid Teflon pulsed plasma thruster*, Air Force Rocket Propulsion Laboratory TR-79-60, NASA CR-162786, Sept., 1979
28) Ruyten, W.M., *Density-conserving shape factors for particle simulations in cylindrical and spherical coordinates*, J. of Comp. Phys., V.105, 1993, pp224-232
29) Samanta Roy, R.I., et al., *A review of contamination from electric propulsion thrusters*, AIAA94-2469,, 1994.
30) Samanta Roy, R.I., Hastings, D.E., Gatsonis, G.A., *Ion-thruster plume modeling for backflow contamination*, J. of Spacecraft and Rockets, V.33, No.4, pp525-534, 1996.
31) Samanta Roy, R.I., Hastings, D.E., Gatsonis, G.A., *Numerical simulation of spacecraft contamination and interactions by ion-thruster effluents*, J. of Spacecraft and Rockets, Vol.33, No.4, pp535-542, 1996.
32) Schunk, R.W., *Mathematical Structure of Transport Equations for Multispecies Flows*, J. Geophys. Res., Vol.15, No.4, 1977, pp. 429-445.
33) Taylor, J.C., Carlson, A.B., Hassan, H.A., *Monte Carlo simulation of radiating re-entry flows*, J. of Thermophysics and Heat Transfer, Vol.8, No.3, 1994, pp478-485.
34) Thomassen, K.I., Vondra, R.J., *Exhaust velocity studies of a solid Teflon pulsed plasma thruster*, AIAA-71-94, 1971.
35) Thomassen, K.I., Tong, D., *Interferometric density measurements in the arc of a pulsed plasma thruster*, J. of Spacecraft, Vol.10, No.3, 1973
36) Vondra, R.J., Thomassen, K.I., Solbes, A., *Analysis of solid Teflon pulsed plasma thruster*, J. of Spacecraft and Rockets, Vol.7, No.12, Dec., 1970
37) Vondra, R.J., Thomassen, K.I., Solbes, A., *A pulsed electric thruster for satellite control*, Proceedings of the IEEE, Vol.59, No.2, Nov., 1971.
38) Woronowicz, M.S., Rault, D.F.G., *On plume flowfield analysis and simulation techniques*, AIAA 94-2048,1994

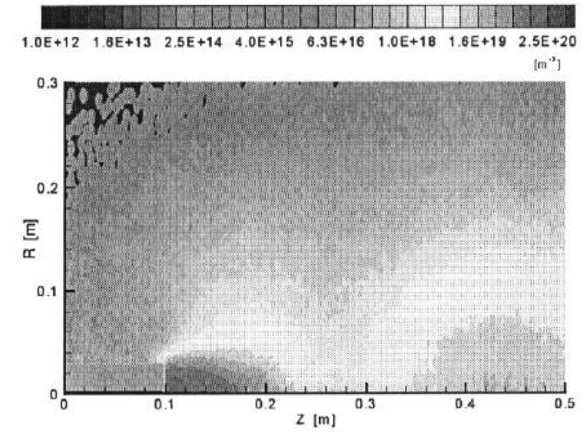

Figure 2: Ion number density at t=12 μs.

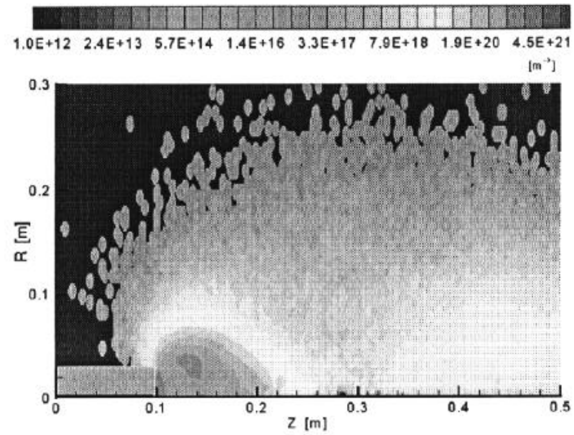

Figure 3: Neutral number density at t=12 μs.

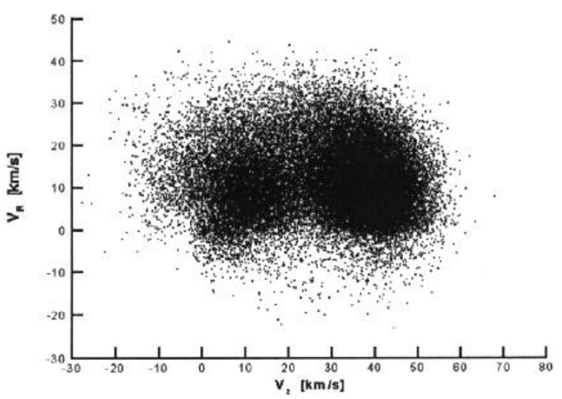

Figure 4: Ion particles phase plot ($V_{iz} - V_{ir}$)

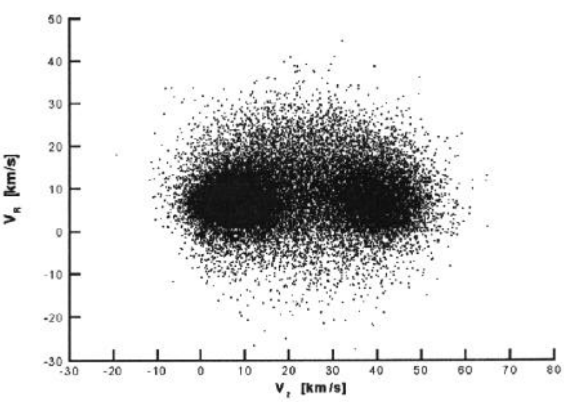

Figure 5: Neutral particles phase plot ($V_{iz} - V_{ir}$)